Tyrosine phosphorylation within the SH3 domain regulates CAS subcellular localization, cell migration, and invasiveness

Radoslav Janoštiak[a], Ondřej Tolde[a], Zuzana Brůhová[a], Marian Novotný[a], Steven K. Hanks[b], Daniel Rösel[a], and Jan Brábek[a]

[a]Department of Cell Biology, Faculty of Science, Charles University, 12843 Prague, Czech Republic; [b]Department of Cell and Developmental Biology, Vanderbilt University Medical Center, Nashville, TN 37232

ABSTRACT **Crk-associated substrate (CAS) is a major tyrosine-phosphorylated protein in cells transformed by v-*crk* and v-*src* oncogenes and plays an important role in invasiveness of Src-transformed cells. A novel phosphorylation site on CAS, Tyr-12 (Y12) within the ligand-binding hydrophobic pocket of the CAS SH3 domain, was identified and found to be enriched in Src-transformed cells and invasive human carcinoma cells. To study the biological significance of CAS Y12 phosphorylation, phosphomimicking Y12E and nonphosphorylatable Y12F mutants of CAS were studied. The phosphomimicking mutation decreased interaction of the CAS SH3 domain with focal adhesion kinase (FAK) and PTP-PEST and reduced tyrosine phosphorylation of FAK. Live-cell imaging showed that green fluorescent protein–tagged CAS Y12E mutant is, in contrast to wild-type or Y12F CAS, excluded from focal adhesions but retains its localization to podosome-type adhesions. Expression of CAS-Y12F in *cas–/–* mouse embryonic fibroblasts resulted in hyperphosphorylation of the CAS substrate domain, and this was associated with slower turnover of focal adhesions and decreased cell migration. Moreover, expression of CAS Y12F in Src-transformed cells greatly decreased invasiveness when compared to wild-type CAS expression. These findings reveal an important role of CAS Y12 phosphorylation in the regulation of focal adhesion assembly, cell migration, and invasiveness of Src-transformed cells.**

Monitoring Editor
Ben Margolis
University of Michigan
Medical School

Received: Mar 10, 2011
Revised: Aug 29, 2011
Accepted: Sep 15, 2011

INTRODUCTION

Crk-associated substrate (CAS) is a major Src substrate implicated in integrin control of cell behavior (reviewed in Defilippi *et al.*, 2006). Reexpression of CAS in *cas*-deficient mouse embryo fibroblasts transformed by oncogenic Src promotes enhanced cell invasiveness, reorganization of actin into large podosome ring and belt structures, activation of matrix metalloproteinase-2, and elevated tyrosine phosphorylation of the focal adhesion proteins focal adhesion kinase (FAK) and paxillin (Brabek *et al.*, 2004). Moreover, CAS signaling is implicated in lung metastasis of Src-transformed mouse embryo fibroblasts (Brabek *et al.*, 2005). The human orthologue of CAS (termed BCAR1, for breast cancer antiestrogen resistance) was identified in a functional screen for genes involved in resistance of breast cancer cells to antiestrogenic drugs (Brinkman *et al.*, 2000). In breast cancer patients, high CAS/BCAR1 levels are associated with early disease recurrence, poor response to tamoxifen treatment, and lower overall survival (Dorssers *et al.*, 2004).

Structurally, CAS is composed of an N-terminal Src homology 3 (SH3) domain that binds to FAK and a C-terminal Src-binding domain (SBD) that includes a binding site for the SH3 domain of Src family of kinases (SFKs; Sakai *et al.*, 1994). The central region of CAS contains a substrate domain (SD), characterized by 15 Tyr-X-X-Pro (YxxP) motifs. SFKs, either directly bound to the CAS SBD or indirectly associated with CAS through a FAK bridge, appear to phosphorylate many or all of the CAS SD YxxP tyrosines (Ruest *et al.*, 2001; Shin *et al.*, 2004).

This article was published online ahead of print in MBoC in Press (http://www.molbiolcell.org/cgi/doi/10.1091/mbc.E11-03-0207) on September 21, 2011.

Address correspondence to: Jan Brábek (brabek@natur.cuni.cz).

Abbreviations used: CAS, Crk-associated substrate; FA, focal adhesion; FAK, focal adhesion kinase; MEF, mouse embryonic fibroblast; SD, substrate domain.

In untransformed cells, phosphorylation of CAS SD tyrosines occurs at sites of integrin-mediated adhesion (Fonseca *et al.*, 2004) and has been linked to integrin signaling pathways regulating cell motility and survival (Klemke *et al.*, 1998; Honda *et al.*, 1999; Cho and Klemke, 2000; Huang *et al.*, 2002). In both cases, recruitment of Crk adaptor proteins to phosphorylated CAS SD YxxP sites is a crucial next step in promoting relevant downstream signaling events, including assembly of a CAS-Crk-DOCK180 scaffold at adhesion sites (Kiyokawa *et al.*, 1998b). Formation of this scaffold drives localized Rac activation (Kiyokawa *et al.*, 1998a), leading to actin polymerization and recruitment of high-affinity integrin receptors necessary for lamellipodia extension and cell migration (reviewed in Burridge and Wennerberg, 2004).

The CAS SH3 domain interacts with polyproline motifs on proteins including FAK (Polte and Hanks, 1995) and PYK2/RAFTK kinases (Li and Earp, 1997), C3G (Kirsch *et al.*, 1998), PTP-PEST (Garton *et al.*, 1997), PTP1B (Liu *et al.*, 1998), CIZ (Nakamoto *et al.*, 2000), and FRNK (Harte *et al.*, 1996). FAK is a prominent focal adhesion protein that interacts with the CAS SH3 domain (Polte and Hanks, 1995, 1997; Harte *et al.*, 1996). This interaction contributes to SD tyrosine phosphorylation by virtue of Src bound to the FAK autophosphorylation site (Ruest *et al.*, 2001). Deletion of the CAS SH3 domain impairs CAS SD tyrosine phosphorylation (Fonseca *et al.*, 2004). In addition to FAK, CAS SH3 domain interacts with tyrosine phosphatases PTP1B (Liu *et al.*, 1998) and PTP-PEST (Garton *et al.*, 1997), suggesting a function for this domain as a molecular switch regulating both CAS phosphorylation and dephosphorylation (Fonseca *et al.*, 2004). Direct interaction of the CAS SH3 domain with C3G might also activate CAS/C3G/DOCK180 signaling (Kirsch *et al.*, 1998). Deletion of the CAS SH3 domain significantly impairs the localization of CAS to focal adhesions (Donato *et al.*, 2010). Phosphoproteomics studies recently identified Tyr-12 (Y12) located within the CAS SH3 domain as a novel site of phosphorylation in Src-transformed mouse embryonic fibroblasts (MEFs) (Luo *et al.*, 2008), although the functional significance of this phosphorylation was not determined.

The objective of this study was to investigate the biological significance of CAS Y12 phosphorylation. A phosphomimicking mutation, Y12E, was found to decrease the SH3 domain-mediated interaction of CAS with FAK and to decrease localization of CAS to focal adhesions (FAs). A nonphosphorylatable Y12F mutation resulted in slower turnover of focal adhesions associated with decreased cell migration in both integrin-dependent and integrin-independent manners. Moreover, expression of CAS Y12F in Src-transformed cells greatly decreased cell invasiveness when compared with wild-type (wt) CAS.

RESULTS

CAS Y12 site is phosphorylated in vivo, and Y12 phosphorylation is elevated in invasive cancer cells

A novel site of tyrosine phosphorylation within the CAS SH3 domain, Tyr-12, was recently identified in a phosphoproteomic analysis of Src-transformed mouse fibroblasts (Luo *et al.*, 2008). To aid in the investigation of CAS Tyr-12 phosphorylation, a phospho-specific antibody was developed against the site. In *cas–/–* MEFs reexpressing CAS, the phospho-specific antibody detected wt CAS but not a mutant in which Tyr-12 was changed to nonphosphorylatable phenylalanine (CAS-Y12F; Figure 1A), thus demonstrating antibody specificity.

The Tyr-12 phospho-specific antibody was further used to confirm the phosphoproteomic analysis data showing the enrichment of Tyr-12 phosphorylation in Src-transformed mouse fibroblasts (Luo *et al.*, 2008). Consistently, the antibody detected high levels of CAS phosphorylated on Tyr-12 in Src-transformed MEFs when compared

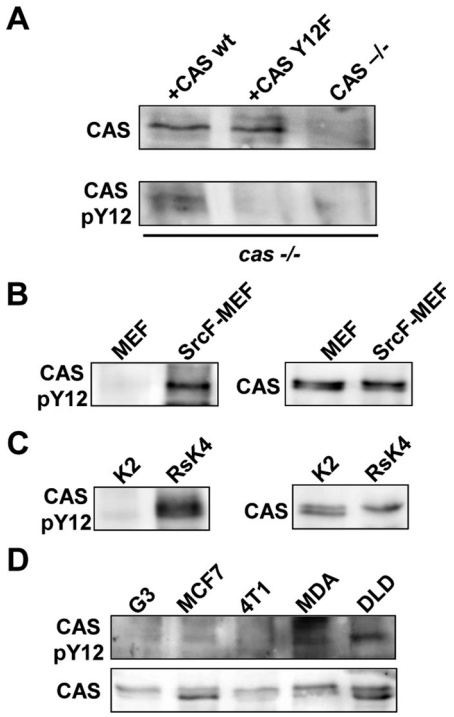

FIGURE 1: CAS is phosphorylated on Tyr-12 in invasive cancer cells. Total cell lysates were analyzed by immunoblotting. Tyr-12 phosphorylation of CAS protein was detected with CAS pY12 phospho-specific antibody in (A) untransformed *cas–/–* MEFs and *cas–/–* MEFs transiently reexpressing CAS Y12F or CAS wt (top; bottom, total CAS levels), (B) untransformed MEFs (MEF) and Src-transformed MEFs (SrcF-MEF), (C) K2 and RsK4 rat sarcoma cells, (D) human breast carcinoma cells lines G3, MCF-7, MDA-MB-231 (MDA), and 4T1 and human colorectal carcinoma line DLD. The immunoblots are representative of at least three independent experiments.

to untransformed MEFs (Figure 1B). The possible role of Src in phosphorylation of CAS on Tyr-12 was further confirmed in a rat fibrosarcoma cellular model of metastasis composed of parental noninvasive K2 cells and derived, highly invasive, Rous sarcoma virus–transformed RsK4 cells (Vesely, 1972). As in Src-transformed MEFs, the v-Src–transformed RsK4 cells exhibited a higher level of CAS phosphorylation on Tyr-12 than did parental nontransformed K2 cells (Figure 1C). Taken together, these data suggest that CAS phosphorylation on Tyr-12 is mediated by activated Src.

To investigate the physiological relevance of Tyr-12 phosphorylation, the level of Tyr-12 phosphorylation was analyzed in set of human carcinoma cell lines. CAS was expressed at similar levels in all cell lines tested (Figure 1D, bottom). The highest level of phosphorylation on Tyr-12 was detected in invasive colorectal carcinoma DLD cells (Figure 1D, top). Out of breast carcinoma cell lines tested, the highly invasive MDA-MB cells exhibited much higher level of Tyr-12 phosphorylation than did noninvasive MCF-7 or EM-G3 (Tolde *et al.*, 2010a) cells (Figure 1D, top). Taken together, these results confirm the biological relevance of Tyr-12 phosphorylation of CAS and suggest that increased phosphorylation of CAS on Tyr-12 may correlate with enhanced invasive behavior.

Phosphorylation of CAS Tyr-12 in the SH3 domain decreases the association with FAK and PTP-PEST

Tyr-12 lies within the first hydrophobic pocket of the SH3-domain ligand-binding surface (Wisniewska *et al.*, 2005), and its

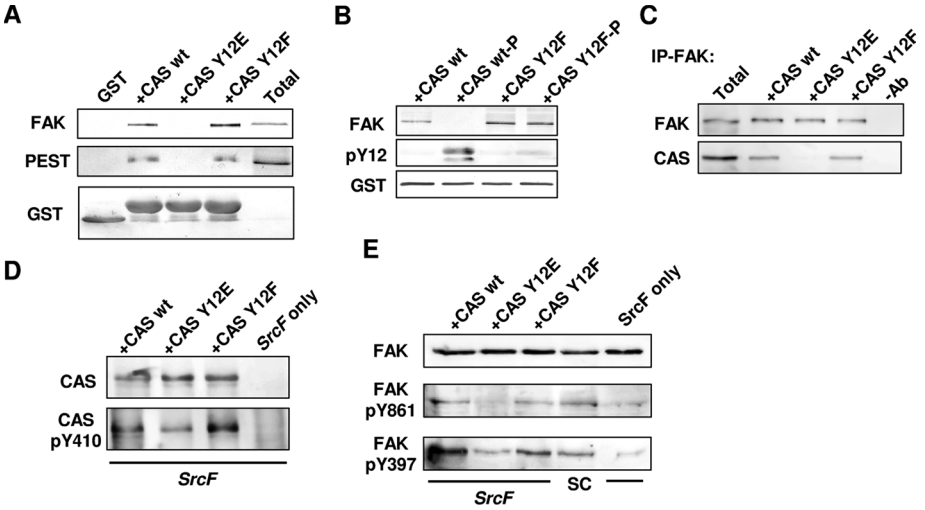

FIGURE 2: The effects of CAS Y12-site mutations on CAS ligand-binding capability and CAS and FAK phosphorylation. (A) Ligand binding of SH3 domains of CAS wt, CAS Y12F, and CAS Y12E fused with GST was analyzed after pull-down assays by immunoblotting. FAK, PTP-PEST, and GST proteins were detected by general anti-FAK, anti–PTP-PEST, and anti-GST antibodies. Aliquots of total cell lysates (Total) were used as controls. (B) Binding of FAK to SH3 domains of CAS wt and CAS Y12F after phosphorylation by Bmx kinase (CAS wt-P, CAS Y12F-P) or without Bmx kinase treatment was detected using general anti-FAK antibody. The phosphorylation and the loading of CAS SH3 domains was documented using CAS pY12 phospho-specific anti-GST antibody, respectively. (C) FAK was immunoprecipitated from *cas–/–* MEFs expressing CAS Y12 variants, and binding of CAS was analyzed using total CAS antibody. (D) Total cell lysates from *cas–/–* MEFs transformed by activated Src (SrcF) expressing CAS wt, CAS Y12F, and CAS Y12E were analyzed by immunoblotting. Total CAS protein was detected with general anti-CAS antibody. Phosphorylation of CAS substrate domain was detected by phospho-specific antibody against Y410. (E) Total cell lysates from *cas–/–* MEFs transformed by activated Src (SrcF) expressing CAS wt, CAS Y12F, CAS Y12, and CAS wt from retroviral vector (SC) were analyzed by immunoblotting. Total FAK protein was detected with general anti-FAK antibody, and tyrosine-phosphorylated FAK was detected with phospho-specific antibodies against Y397 or Y861.

phosphorylation could thus potentially affect ligand-binding capacity. To analyze the role of Tyr-12 phosphorylation in regulating binding capacity of the CAS SH3 domain, mutational variants with either the nonphosphorylatable Y12F substitution or a phosphomimicking Y12E substitution (Tyr-12 changed to glutamic acid) were prepared as glutathione *S*-transferase (GST)–SH3 fusion proteins. Pull-down assays were performed to analyze the association of the SH3-domain variants with FAK and PTP-PEST, which both can bind directly to the CAS SH3 domain to regulate tyrosine phosphorylation of the CAS SD. As expected, the wt SH3 domain effectively recovered both FAK and PTP-PEST from HeLa cell lysates, as did the structurally similar Y12F substitution (Figure 2A). However the Y12E substitution showed no detectable association with either FAK or PTP-PEST (Figure 2A), indicating that phosphorylation of Tyr-12 effectively disrupts the SH3-domain binding capacity. To confirm this, the wt versus Y12F SH3 variants were subjected to phosphorylation in vitro and tested for their abilities to bind to FAK in the pull-down assay. Recombinant Bmx kinase was found to effectively phosphorylate the wt CAS SH3 domain on Tyr-12 (Figure 2B) and thus was used in the phosphorylation reaction. Recombinant Src kinase was also able to phosphorylate the CAS SH3 domain, although less effectively than the Bmx preparation (unpublished data). Similar to the Y12E substitution, phosphorylation of the wt SH3 domain resulted in a loss of association of the SH3 domain with FAK (Figure 2B). The Y12F SH3 domain variant was not phosphorylated by Bmx on Tyr-12 (Figure 2B), and consequently the treatment with Bmx did not alter its capacity to bind FAK. To confirm that the Y12E substitution affects also the ability of full-length CAS to interact with FAK, FAK was immunoprecipitated from *cas–/–* MEFs expressing CAS Y12 variants, and binding of CAS was analyzed using total CAS antibody. Consistent with the results of pull-down assays, CAS Y12E substitution resulted in a great decrease of association with FAK (Figure 2C and Supplemental Figure S1A).

The CAS Y12F substitution increases tyrosine phosphorylation of the CAS substrate domain, and the Y12E substitution decreases tyrosine phosphorylation of FAK

The foregoing findings indicate that CAS Tyr-12 phosphorylation might be critically involved in regulating CAS signaling functions. To further test this notion, cell lines were prepared to stably express full-length CAS variants: wt, Y12E, or Y12F. The variants were expressed from a CMV-based plasmid in both normal and Src-transformed *cas–/–* MEFs. In the Src-transformed cells, the Y12F substitution resulted in a significant increase in SD tyrosine phosphorylation as assessed by pY410 antibody. The Y12E substitution consistently resulted in slightly decreased tyrosine phosphorylation of the SD when compared to wt CAS, though the decrease was not statistically significant (Figure 2D and Supplemental Figure 1B).

The effects of the CAS Y12 substitutions on FAK tyrosine phosphorylation were also investigated. Replicate blots were probed with FAK antibody and phospho-specific antibodies against major FAK phospho-acceptor tyrosines. As previously reported (Brabek *et al.*, 2004), wt CAS expression enhanced FAK tyrosine phosphorylation in Src-transformed cells of both Tyr-861 (the major C-terminal Src site) and Tyr-397 (the major autophosphorylation site; Figure 2E, compare first and last lanes). The CAS-Y12F variant also was able to enhance FAK tyrosine phosphorylation, although not to the same extent as wt CAS. However, CAS-Y12E was unable to promote FAK tyrosine phosphorylation above the basal level seen in the absence of CAS expression (Figure 2E and Supplemental Figure S1C). Taken together, these results suggest that inhibition of CAS SH3-domain binding capacity through Y12-site phosphorylation results in slightly decreased CAS-mediated tyrosine phosphorylation of FAK.

The Y12E substitution decreases the localization of CAS into focal adhesions but not into podosome-type adhesions

Because the CAS SH3 domain has a role in targeting the protein to focal adhesions (Donato *et al.*, 2010), the Y12 substitutions were further tested for their abilities to influence subcellular localization. To analyze localization, full-length CAS Y12-site substitution variants were expressed with an N-terminal green fluorescent protein (GFP) tag in RsK4 sarcoma cells. RsK4 cells are transformed by v-Src and exhibit pronounced focal and podosome-type adhesions (PTAs; Tolde *et al.*, 2010b). GFP-CAS localization was assessed by fluorescence confocal microscopy. Localization of GFP-CAS to focal or podosome-type adhesions was examined by differential

colocalization with phosphorylated FAK or phosphorylated cortactin, respectively. Focal adhesions were identified as elongated structures at the cell periphery with a uniform colocalization of phosphorylated FAK and F-actin. Podosome-type adhesions were identified as rounded structures at the ventral surface with central staining for phosphorylated cortactin. In comparison to wt GFP-CAS, the Y12E variant was significantly impaired in its ability to localize into focal adhesions (Figure 3, A and B). The GFP-CAS Y12E was found only in 34% of focal adhesions (Figure 3B, left); moreover the relative intensity of GFP-CAS Y12E signal in focal adhesions was slightly, albeit not significantly ($p = 0.053$) lower than the signal of GFP-CAS wt (Figure 3B, right). The Y12F substitution had no effect on GFP-CAS localization in focal adhesions (Figure 3, A and B). The same defect in focal adhesion localization for the Y12E variant was observed in nontransformed MEFs (Supplemental Figure S2). Remarkably, neither the Y12E nor the Y12F substitution had any influence on the GFP-CAS localization into podosome-type adhesions (Figure 3, A and C). The GFP-CAS wt, Y12F, and Y12E variants were all been confirmed to associate with active podosome-type adhesions as evidenced by their colocalization with sites of gelatin degradation (Figure 3C). Thus the phosphomimicking Y12E substitution has a differential effect on the ability of CAS to localize into focal adhesions and podosome-type adhesions. To extend the evidence that phosphorylation of CAS Y12 decreases CAS localization to focal adhesions, the cells were analyzed for staining with the Tyr-12 phospho-specific antibody. The antibody did not recognize either Y12F or Y12E variants, as its signal in the *cas–/–* cells expressing those variants was very low and uniform (Supplemental Figure S3). In contrast, in *cas–/–* cells expressing the wt CAS the pY12 signal was enriched in FAs. However, only a minor part of GFP-CAS positive focal adhesions was stained with pY12 antibody (Supplemental Figure S3A), consistent with decreased localization of phosphomimicking Y12E variant to FAs (Figure 3A). Furthermore, in Src-transformed *cas–/–* cells expressing CAS wt the Tyr-12 phospho-specific antibody stained large podosomal aggregates (Supplemental Figure S3B), as described in these cells previously (Brabek *et al.*, 2004).

These results confirm the previously recognized role of the CAS SH3 domain in CAS localization into FAs and suggest that phosphorylation of the CAS Y12 site could result in releasing CAS from FAs.

The Y12 variants differentially affect cell migration and adhesion

Because the CAS Y12E substitution resulted in decreased localization into focal adhesions, it was of interest to examine whether the Y12 substitution variants influenced cell migration. To analyze cell migration, wound-healing assays were performed on *cas–/–* parental cells versus cells expressing either wt CAS or Y12 substitution variants (Supplemental Figure S4A). The percentage wound coverage was determined after 12 h. As previously reported (Huang *et al.*, 2002; Shin *et al.*, 2004; Meenderink *et al.*, 2010), wt CAS expression significantly enhanced the wound-healing migration on fibronectin in comparison to the parental cells lacking CAS (Figure 4A and Supplemental Figure S4B). The CAS-Y12E variant promoted the wound-healing cell migration response to a degree even greater than wt CAS (Figure 4A). In contrast, cells expressing CAS-Y12F had a very poor migration response when compared to wt CAS—even lower than that of the *cas–/–* cells (Figure 4A). On polylysine-coated dishes, where cell adhesion is independent of integrins, wt CAS did not promote the cell migration response (Figure 4B).

Of interest, the migration-enhancing effect of CAS-Y12E was even more pronounced on polylysine (Figure 4B). The CAS-Y12F variant had a small but significant inhibitory effect on migration on the polylysine surface (Figure 4B). Thus the Y12E substitution leads to enhanced cell migration in a manner largely independent of integrin-mediated adhesion, whereas the Y12F substitution leads to decreased migration in both integrin-dependent and integrin-independent manners. Similar to results obtained in nontransformed cells, in Src-transformed cells CAS-Y12E enhanced migration on polylysine relative to wt CAS, whereas CAS-Y12F had a mild inhibitory effect, although the decrease was not statistically significant ($p = 0.06$; Figure 4C). To further analyze the effect of CAS Y12 variants on motility of Src-transformed cells, Boyden chamber chemotaxis assays were performed. Consistent with results obtained in wound-healing assays, in Src-transformed cells CAS-Y12E greatly enhanced chemotaxis toward 10% fetal bovine serum (FBS) relative to wt CAS (Figure 4D).

Studies have linked CAS SD hyperphosphorylation to increased cell adhesiveness (Angers-Loustau *et al.*, 1999; Kira *et al.*, 2002; Siesser *et al.*, 2008). Because the Y12F substitution was found to enhance CAS SD tyrosine phosphorylation, we further analyzed the effect of the Y12 substitution variants on the spreading of Src-transformed cells. Indeed, the CAS-Y12F variant was found to result in slight, albeit not statistically significant, increase in cell spreading on polylysine in comparison to wt (Figure 4E). Of interest, CAS-Y12E was found to greatly decrease cell spreading on both polylysine and fibronectin (Figure 4, E and F), suggesting that this function depends on the SH3-domain binding capacity. These results suggest that CAS Y12-site phosphorylation results in enhanced cell migration and decreased cell spreading.

The Y12E and Y12F variants differentially affect CAS-enhanced cell invasiveness and the activity of extracellular proteases

Having established the critical importance of the CAS Y12 phosphorylation site for cell migration, we next analyzed whether this site also influences the invasive behavior of Src-transformed cells in a three-dimensional environment. Similar to results from the migration assays, when compared to wt CAS, CAS-Y12E slightly increased the invasiveness of Src-transformed cells in three-dimensional collagen (Figure 5A). However, CAS-Y12F resulted in profound decrease in cell invasiveness, to levels comparable to the Src-transformed parental cells lacking CAS (Figure 5A).

Invasiveness of Src-transformed cells was previously found to be associated with expression and activation of matrix metalloproteinases (Brabek *et al.*, 2004). To analyze whether the CAS Y12 substitutions affect expression and production of matrix metalloproteinases, the cells were plated on Alexa 633 gelatin and cell-associated gelatinase activity was detected by localized loss of Alexa 633 fluorescence. This in situ assay effectively detects either secreted or membrane-bound gelatinase activity. We found gelatinase activity to be substantially increased in cells expressing the CAS Y12E substitution when compared to wt CAS or Y12F variants (Figure 5, B and C). Thus the differences in invasion potential of cells expressing the Y12 variants appear to be at least partially caused by differences in gelatinase activity. These results show that inhibition of CAS Y12-site phosphorylation results in decreased cell invasiveness.

The Y12F substitution results in decreased turnover of focal adhesions, and the Y12E substitution increases turnover of CAS in podosome-type adhesions

As suggested by the pronounced effects of the Y12 variants on cellular migration, the differences in invasion potential of the CAS Y12 variant cell lines could be also due to differences in turnover of focal

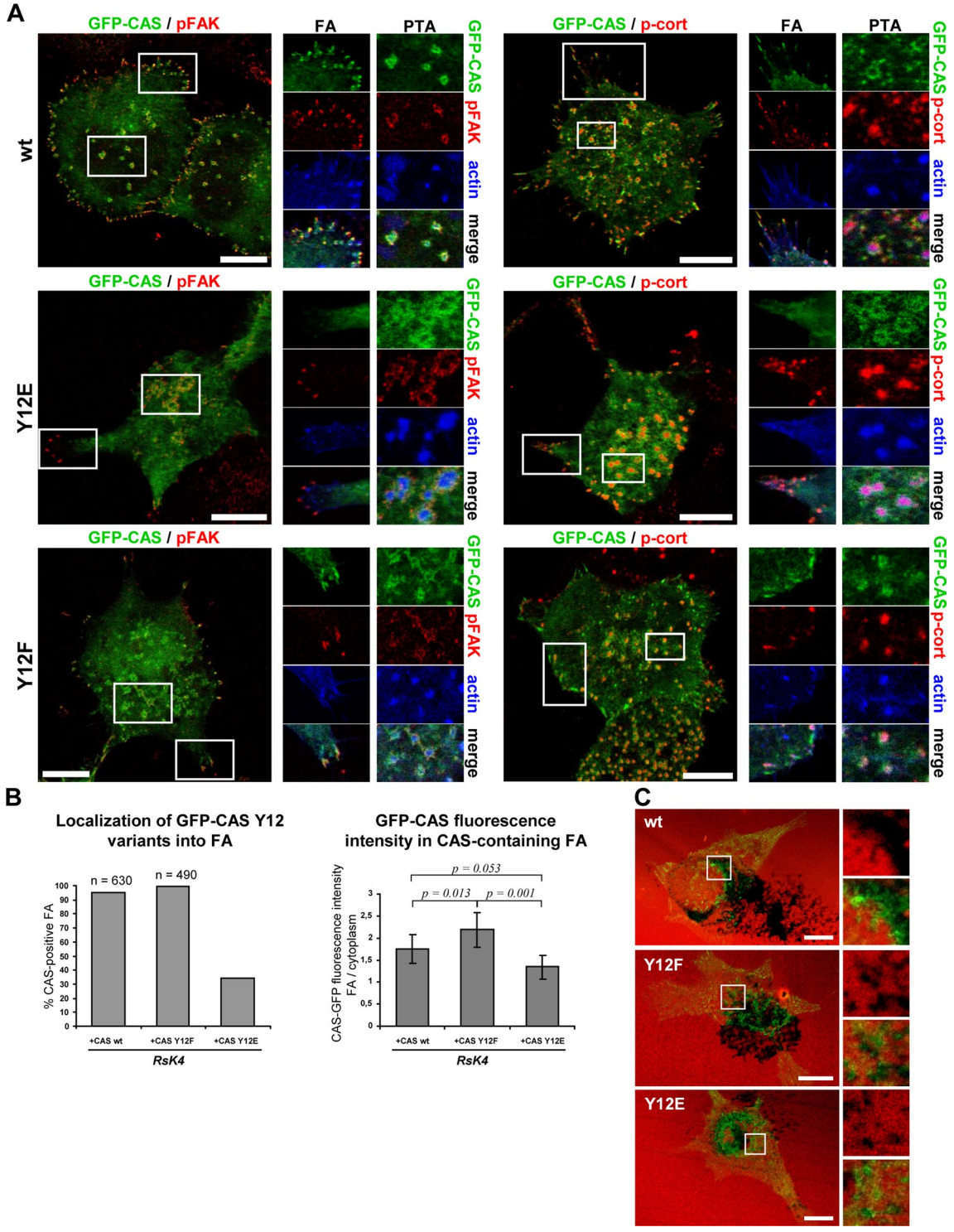

FIGURE 3: CAS Y12E mutation results in decreased localization of CAS into focal adhesions but not into podosome-type adhesions. CAS wt, Y12F, and Y12E cells were grown on fibronectin-coated coverslips. (A) RsK4 cells expressing GFP-CAS (green) were stained for F-actin (blue) and either phospho-FAK (red; left) or phosphocortactin (red; right). Details, as indicated in larger images, show several FA (left) and PTA (right) structures. (For Y12F mutant, phosphocortactin staining of focal adhesions, right images are rotated 90° relative to boxed area on the left.) (B) Left, indicated number, n, of FAs in RsK4 cells expressing CAS variants were analyzed for the presence of GFP-CAS. The histogram bars represent the percentage of FAs positive for GFP-CAS. Right, in GFP-CAS-positive FAs, the average fluorescence intensity of GFP signal in FAs was compared to average fluorescence intensity of the GFP signal in cytoplasm. The histogram bars represent the average ratio of fluorescence intensity of GFP signal in FAs vs. cytoplasm, with error bars representing standard deviations and p values indicating statistical significance. The data were obtained from a minimum of 30 cells in three independent experiments. (C) RsK4 cells expressing GFP-CAS (green) were plated on Alexa 633–stained gelatin (red); the areas of gelatin degradation are black. Right, details show colocalization of PTA structures with sites of gelatin degradation. Scale bars,10 μm.

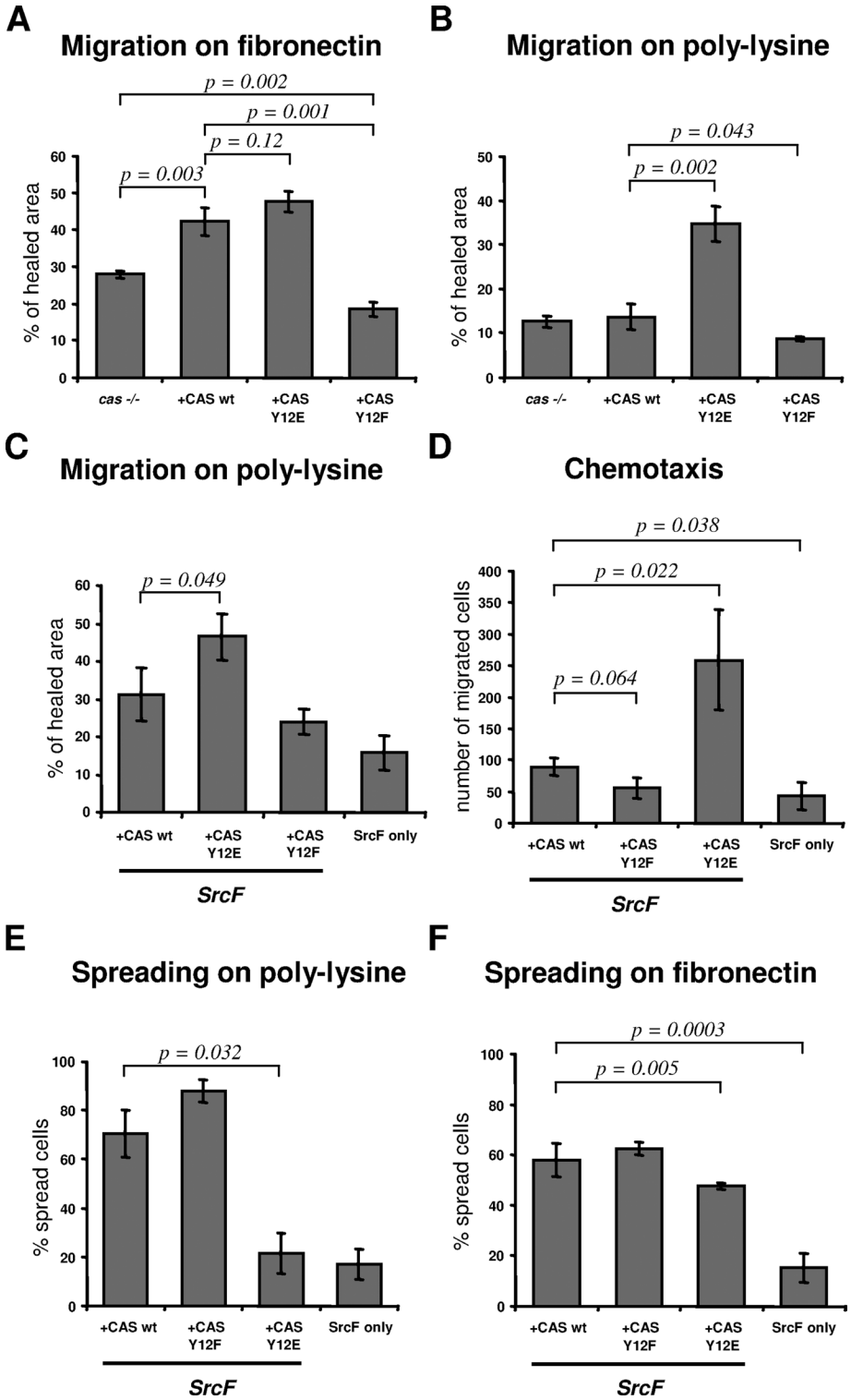

FIGURE 4: Effect of CAS Y12-site mutations on motility of mouse embryonic fibroblasts. (A) *cas–/–* MEFs expressing indicated CAS variants (wt, Y12E, and Y12F) were allowed to migrate for 12 h on either polylysine- or 10 µg/ml fibronectin–coated wells using the Oris Cell Migration Assay as described in *Material and Methods*. (B) *cas–/–* MEFs expressing CAS variants were allowed to migrate for 12 h on polylysine-coated, 35-mm µ-Dish with Ibidi Culture-Insert. The distance migrated by the cells was monitored over a period of time by observation with Nikon Eclipse TE2000-S. (C) Src-transformed *cas–/–* MEFs (SrcF) expressing CAS variants (wt, Y12E, and Y12F) were allowed to migrate for 12 h on polylysine-coated, 35-mm µ-Dish with Ibidi Culture-Insert. For A–C, histogram bars represent migration rates obtained from three independent experiments, with error bars representing standard deviations and p values indicating statistical significance. (D) Src-transformed *cas–/–* MEFs (SrcF) expressing CAS variants (wt, Y12E, and Y12F) were analyzed using Boyden chamber chemotaxis assay toward 10% FBS. The cells were allowed to chemotax for 10 h. The histogram bars show average numbers of transmigrated cells obtained from three independent experiments, with error bars representing standard deviations and p values indicating statistical significance. (E, F) The effect of CAS Y12-site mutants on cell spreading. (E) Src-transformed *cas–/–* MEFs (SrcF) expressing wt CAS or CAS Y12 mutants were allowed to spread on polylysine-coated tissue culture dishes, and the number of spread cells was assayed after 120 min. A quantitative evaluation was expressed as the number of cells spread as a percentage of the total number of cells in the field. Average number of cells per field, 200. (F) Src-transformed *cas–/–* MEFs (SrcF) expressing wt CAS or CAS Y12 mutants were allowed to spread on fibronectin-coated tissue culture dishes, and the number of spread cells was assayed after 120 min. A quantitative evaluation was expressed as the number of cells spread as a percentage of the total number of cells in the field. Average number of cells per field, 400. For E and F the histogram bars represent the mean percentage of spreading from three replicate assays, with error bars representing standard deviations and p values indicating statistical significance.

adhesions required for cellular motility. To test this hypothesis, the mean size of ventral adhesion structures as revealed by fluorescence microscopy was determined. This analysis revealed a difference in the size of the cellular adhesion structures formed in the cells expressing the different CAS Y12 variants. Whereas the adhesions of the cells expressing the Y12E variant were similar in size relative to those of wt CAS cells, the mean adhesion size of the CAS-Y12F cells was significantly larger than that of the wt and Y12E-expressing cells (Figure 6A).

To further confirm the differences in FA dynamics, live-cell microscopy was performed on Src-transformed MEFs coexpressing individual CAS Y12 variants together with mCherry-vinculin as a marker of FAs. FAs assembly and disassembly rates were measured for all variants. Consistent with the observed differences in FA size, cells expressing CAS Y12F mutation were found to have slower rates of both FA assembly (Figure 6B, left) and FA disassembly (Figure 6B, right).

The dynamic exchange of vinculin in focal adhesions decreases during adhesion maturation (Mohl *et al.*, 2009). FRAP was used to determine whether the different

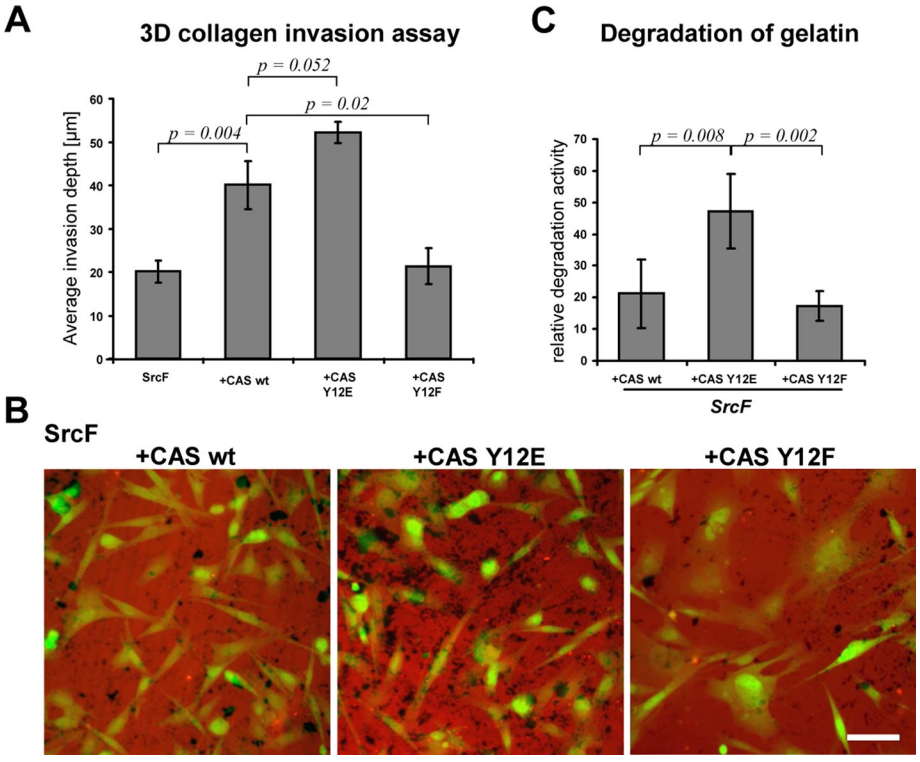

FIGURE 5: CAS Y12F mutation results in decreased invasiveness of Src-transformed cells. (A) Three-dimensional collagen invasion assay. *Cas–/–* MEFs transformed by activated Src (SrcF) expressing CAS wt, CAS Y12F, and CAS Y12E were seeded on top of the collagen gel and their invasion was scored as described in *Materials and Methods*. The histogram bars represent the mean percentage of invasion from three independent experiments, with error bars representing standard deviations and p values indicating statistical significance. Total number of cells counted was as followed: *cas–/–* SrcF, 116; +WT, 266; +YE, 311; +YF, 196. (B) Gelatin degradation assay. Src-transformed MEFs cells expressing indicated GFP-CAS variant (green) were plated on Alexa 633–stained gelatin (red); the areas of degradation are black. Representative images are shown. Scale bars, 50 μm (C) Quantification of the gelatin degradation assay (B). The histogram bars represent the mean percentage of relative degradation activity calculated as degraded area divided by area occupied by cells from three replicate assays, with error bars representing standard deviations and p values indicating statistical significance.

CAS Y12 variants had an effect on vinculin exchange dynamics. Src-transformed *cas–/–* parental cells and cells expressing the CAS Y12 variants were transiently transfected to express YFP-vinculin, and the exchange rates of YFP-vinculin in mature focal adhesions at the periphery of the cells were determined. The fluorescence recovery after photobleaching (FRAP) experiments revealed a much higher recovery half-life for vinculin in cells expressing the Y12F variant (24.5 ± 5 s) than in cells expressing wt CAS (14.6 ± 2.5 s; wt vs. Y12F, p = 0.0007) or the Y12E variant (9.5 ± 3.7 s; wt vs. Y12E, p = 0.014; Figure 6C). The higher vinculin recovery half-life observed in cells expressing the Y12F variant correlates with the larger mean adhesion size in these cells and is indicative of a defect in focal adhesion disassembly. On the other hand, vinculin has a shorter recovery half-life in the cells expressing CAS-Y12E and an almost 100% mobile fraction, which is consistent with the smaller adhesion size and could indicate a short adhesion lifetime.

We further assessed whether the Y12F substitution could influence the exchange dynamics of GFP-CAS in focal adhesions. Instead of Src-transformed *cas–/–* MEFs, which express cytoplasmic GFP, Src-transformed RsK4 cells were used for FRAP analysis of the GFP-CAS variants. The recovery half-life of CAS in focal adhesions was found to be comparable for both wt (4.2 ± 1.3 s) and Y12F (4.3 ± 1.6, wt vs. Y12F, p = 0.86) variants (Figure 6D). However the percentage recovery was significantly decreased for the Y12F variant (38 vs. 75% for wt; Figure 6D) suggesting that a much larger fraction of the CAS-Y12F variant is stably bound within focal adhesions in comparison to the wt. The Y12E variant was not tested in the FRAP analysis of focal adhesions because it is excluded from focal adhesions.

Because CAS Y12-site substitutions greatly affected the invasion potential of Src-transformed cells, it was of interest to determine whether the substitutions also influenced the recovery half-life of CAS within podosome-type adhesions. The recovery half-life in podosome-type adhesions was found to be significantly lower for the Y12E variant (1.5 ± 0.4 s) than in the CAS wt (4.8 ± 2.3 s, wt vs. Y12E, p = 0.0052) or Y12F (3.7 ± 1.2 s, wt vs. Y12F, p = 0.18; Figure 6E), suggesting that the phosphomimicking Y12E mutation greatly increases CAS dynamics within podosome-type adhesions.

DISCUSSION

In this study we showed that phosphorylation of Tyr-12 in the CAS SH3 domain disrupts the SH3 binding function. Blocking the capacity for Tyr-12 phosphorylation through phenylalanine substitution resulted in cells having abnormally large focal adhesions and decreased FA dynamics and exhibiting defects in cell migration in both two- and three-dimensional environments. Moreover, substitution of Tyr-12 with glutamate to mimic the negative charge of the phosphate group resulted in increased cell motility. Thus we identified a new mechanism for the functional regulation of CAS.

Tyrosine phosphorylation within SH3 domains is gaining increased recognition as an important mechanism for regulating signaling proteins. CAS Tyr-12 lies within the first hydrophobic pocket of the SH3-domain surface involved in ligand interaction. Homologous tyrosine residues in SH3 domains in other proteins, including Btk (Park *et al.*, 1996), Syk, (Morrogh *et al.*, 1999), and Abl (Meyn *et al.*, 2006; Chen *et al.*, 2008), have been shown to be subject to phosphorylation and disruption of SH3 binding function. These studies provided substantial evidence for a significant role of phosphorylation on well-conserved tyrosines within SH3-domain hydrophobic pockets on the binding capacity of the SH3 domain.

CAS was found to promote both migration and invasiveness of transformed cells (Brabek *et al.*, 2004, 2005). Reexpression of CAS in *cas*-deficient mouse embryo fibroblasts transformed by oncogenic Src promoted an invasive phenotype associated with enhanced cell invasiveness, reorganization of actin into large podosome ring and belt structures, activation of matrix metalloproteinase-2, and elevated tyrosine phosphorylation of the focal adhesion proteins FAK and paxillin. The SH3 domain of CAS was important for all of these processes but was not required for formation of large podosome structure. Efficient metalloproteinase activation involving CAS SH3 domain–mediated signaling and enhanced podosome

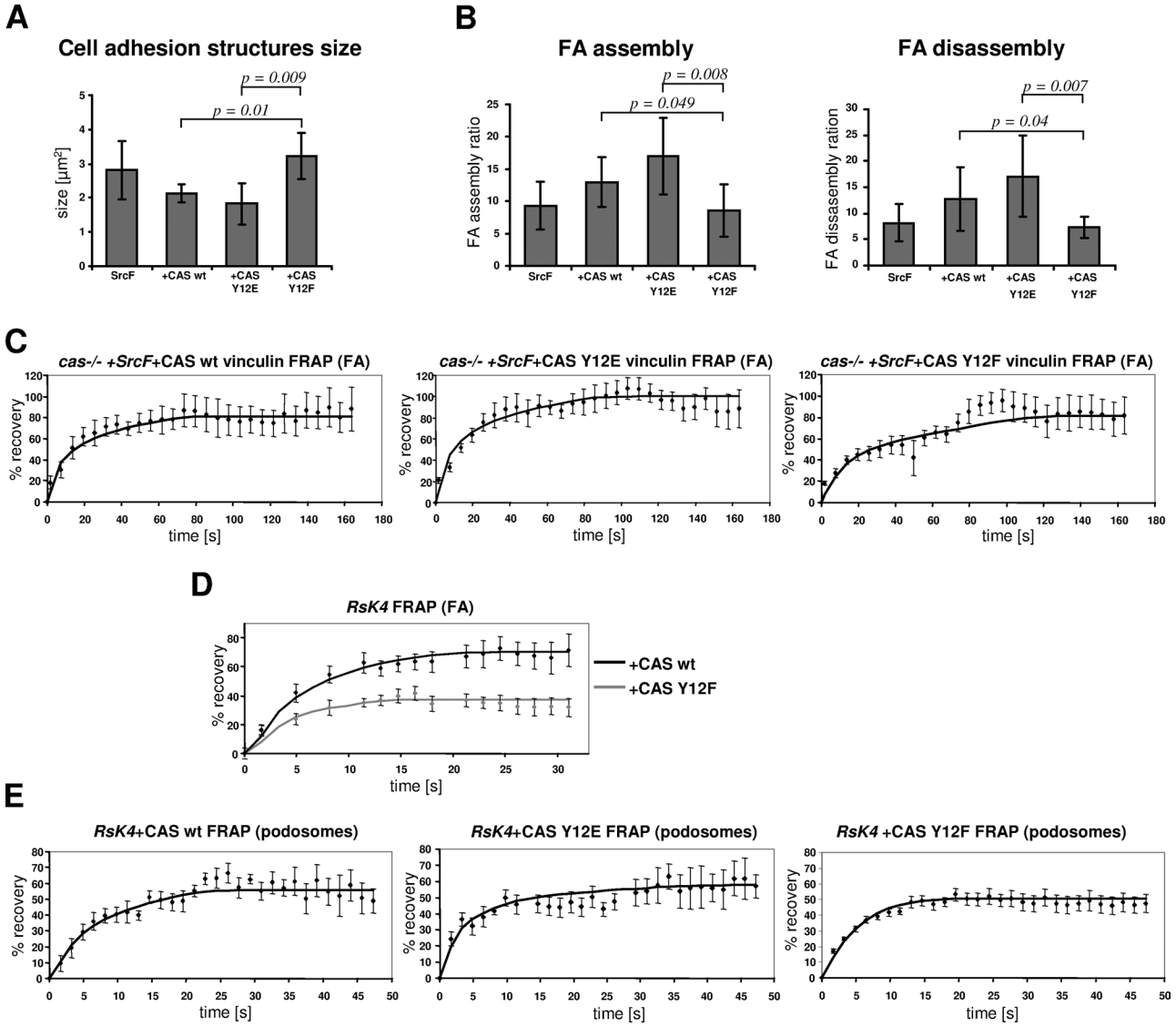

FIGURE 6: Effects of CAS Y12-site mutations on dynamics of focal adhesions and podosome-type adhesions. (A) Quantification of cellular adhesion structure size in *cas–/– + SrcF* MEFs expressing indicated CAS variant and mCherry-vinculin as a marker of FAs using confocal fluorescence microscopy. Columns represent average area of focal adhesion in one cell. The data are shown as an average size of FA ± standard deviation obtained from analyses of 10 cells in three independent experiments. The p values indicate statistical significance. (B) FA dynamics. Live microscopy of Src-transformed MEFs (SrcF) expressing indicated CAS variants together with mCherry-vinculin as a marker of FAs was performed, and FA assembly (left) and disassembly rates (right) were calculated for all variants. The histogram bars represent the mean number of assembled or disassembled FAs per cell during a 60-min period, with error bars representing standard deviations and p values indicating statistical significance. Ten cells per indicated cell line were analyzed in three independent experiments. (C) FRAP curves of vinculin-YFP associated with focal adhesions in Src-transformed MEFs (SrcF) expressing indicated variants of CAS protein. Cells were subjected to FRAP analysis 24 h after plating on 10-µg/ml fibronectin–coated wells at 37°C using 63×/1.45 oil objective. After photobleaching, fluorescence recovery was recorded at 6-s intervals. (D) FRAP curves of GFP-CAS variants in FAs of RsK4 cells. Cells were subjected to FRAP analysis 24 h after plating on 10-µg/ml fibronectin–coated wells at 37°C using 63×/1.45 oil objective. After photobleaching, fluorescence recovery was recorded at 1.6-s intervals. (E) FRAP curves of GFP-CAS variants in podosome-type adhesions. FRAP experiments were performed the same way as FRAP experiments in RsK4 cells, but bleached regions were podosome-type adhesions instead of FAs. For all FRAP experiments, the data are shown as an average of 10 independent experiments, with error bars representing standard errors.

assembly involving CAS SD tyrosine phosphorylation are both likely to be important for CAS-mediated invasiveness. Consistent with these assumptions, we found greatly elevated gelatin-degrading capability in Src-transformed cells expressing CAS Y12E mutant when compared to cells expressing CAS wt or Y12F mutant. Thus increased invasion potential of CAS Y12E mutant could be caused at least in part by elevated activation of matrix metalloproteinases.

Although it is recognized that CAS localizes to FAs, where it engages in integrin-mediated signaling via tyrosine phosphorylation (Nojima *et al.*, 1995; Vuori and Ruoslahti, 1995), the dynamics of

CAS targeting to these sites remains poorly understood. CAS arrives early during the assembly of FAs and departs late during FA disassembly (Donato *et al.*, 2010). The early localization of CAS to assembling FAs supports the notion that CAS engages in signaling at the leading edge of migrating cells to promote plasma membrane protrusion. During FA disassembly, CAS appears to persist longer than paxillin. This persistence is supportive of a proposed role for CAS in promoting FA disassembly (Webb *et al.*, 2004). Consistent with these observations, our data show that blocking the capacity for Tyr-12 phosphorylation through phenylalanine substitution results in slower rate of both FA assembly and, to even greater extent, FA disassembly, suggesting the promoting effect of Y12 phosphorylation on FA turnover. Notably, the slower turnover rate of FA in CAS Y12F mutant is associated with hyperphosphorylation of CAS SD, the association that was also observed in PTP-PEST–null cells (Angers-Loustau *et al.*, 1999) and STAT3-null cells (Kira *et al.*, 2002) and cells expressing FAK/Src chimera (Siesser *et al.*, 2008). In all these studies, these phenomena were associated with increased cell adhesiveness and reduced cell motility. We therefore propose that reduced migration and invasiveness of CAS Y12F mutant is caused by decreased rate of FA turnover.

Knowing the subcellular location of signaling-competent CAS molecules would provide valuable insight into the regulation and biological role of CAS signaling. Remarkably, we found that CAS Y12E mutation results in decreased localization of CAS into FAs but not into podosome-type adhesions (Figure 3, A and C). Consistent with these results, the CAS Tyr-12 phospho-specific antibody clearly stained podosome-type adhesions but was mostly excluded from FAs (Supplemental Figure S2). The recent study by Donato *et al.* (2010) clarified the domain requirements for FA targeting of CAS and clearly showed that both the N-terminal SH3 and C-terminal CCH domains are necessary for CAS to properly localize to FAs. The data obtained in our study suggest the possible role of tyrosine phosphorylation within CAS SH3 domain as a mechanism that could regulate the presence of CAS in FAs. Chan *et al.* (2009) observed that FAK depletion switches phosphotyrosine-containing proteins, including CAS, from focal adhesions to invadopodia through the temporal and spatial regulation of c-Src activity. The decreased association of CAS with FAK in the CAS Y12E mutant might similarly account for the reduction of CAS localization at FAs.

Localization of CAS in podosomes was first described by Nakamoto *et al.* (1997). They found that CAS translocates to the podosomes as a result of the introduction of activated Src. The CAS mutants with impaired binding of Src were not localized to podosomes, whereas CAS wt was located predominantly in podosomes. However, staining in podosomes was not detected in the 3T3-aSrc (Src-transformed 3T3) cells expressing the deltaSH3 mutant. These results suggested that the SH3 domain of CAS is essential and the Src-binding domain is also important for the recruitment of CAS to podosomes. Of interest, we observed that CAS harboring the Y12E mutation in the SH3 domain retains its ability to localize in podosome-type adhesions, suggesting that rather than Y12-site phosphorylation status, integrity of the SH3 domain is important for CAS localization to podosome–type adhesions. In our study we did not observe the effect of CAS Y12-site mutations on CAS localization within podosome structures; however, we did see great increase of CAS dynamics within podosome-type adhesions in the CAS Y12E mutant.

Further studies need to be done to find a kinase responsible for CAS Y12 phosphorylation and to elucidate in detail the mechanism of Y12-site phosphorylation regulation. Our data suggest that Src or Bmx could be among the candidates responsible for CAS Y12-site phosphorylation. This is further supported by previously published data, which extensively document CAS phosphorylation by Src (Vuori *et al.*, 1996; Ruest *et al.*, 2001) and also suggest a Tec family member, Bmx, as a possible kinase for CAS (Abassi *et al.*, 2003). Moreover, another Tec family kinase, Itk, was shown to be capable of autophosphorylation on homologous Tyr-180 within its SH3 domain (Joseph *et al.*, 2007).

Taken together, our observations imply an important role of tyrosine phosphorylation in the first binding pocket of the CAS SH3 domain for CAS localization, turnover of adhesion structures, migration, and invasiveness of Src-transformed cells. We hypothesize that CAS Y12 phosphorylation might represent a novel regulatory mechanism by which the CAS-mediated signaling can be altered to trigger different cellular responses. Clarifying the specific role of Y12 for CAS-mediated oncogenic potential may bring new insight into the complex process of cell transformation.

MATERIALS AND METHODS

Cell transfection and culture

cas–/– MEFs expressing constitutively active mouse Src Y529F (SrcF cells) or both SrcY529F and wt CAS (SC cells) were prepared using the LZRS-MS-IRES-GFP retroviral vector and the Phoenix E packaging line as described previously (Brabek *et al.*, 2004). RsK4 cells were transfected with pEGFP-C1-CAS using Lipofectamine 2000 reagent (Life Technologies, Carlsbad, CA) as specified by the manufacturer. *cas–/–* MEFs were transfected with pEGFP-C1 CAS or pIRES-puro-CAS using Lipofectamine 2000. Src-transformed *cas–/–* MEFs were transfected with plasmids pIRES-puro-CAS or yellow fluorescent protein (YFP)–vinculin using Lipofectamine 2000. Stable transfectants were obtained using puromycin selection (3 μg/μl). All cells were cultivated in full DMEM (Life Technologies) with 4500 mg/l L-glucose, L-glutamine, and pyruvate, supplemented with 10% fetal bovine serum (Sigma-Aldrich, St. Louis, MO), 2% antibiotic–antimycotic (Life Technologies), and 1% MEM nonessential amino acids (Life Technologies).

Immunoblotting and immunoprecipitation

Subconfluent cell cultures were washed with phosphate-buffered saline (PBS) and lysed in modified RIPA buffer (0.15 M NaCl; 50 mM Tris-HCl, pH 7.4; 1% Nonidet P-40; 0.1% SDS; 1% sodium deoxycholate; 5 mM EDTA; 50 mM NaF). Protein concentrations in the lysates were determined using the DC Protein Assay (Bio-Rad, Hercules, CA). Protein lysates were diluted in Laemmli sample buffer (0.35 M Tris-HCl, pH 6.8; 10% SDS; 40% glycerol; 0.012% bromophenol blue). For immunoblotting, samples were separated on 10% SDS-polyacrylamide gels and transferred onto nitrocellulose membrane. Nonspecific activity was blocked by incubating membranes for 45 min at 37°C in Tris-buffered saline containing 4% bovine serum albumin. Membranes were then incubated overnight at 4°C with primary antibody, washed extensively with Tris buffered saline with Tween-20 (TTBS), and then incubated for 1 h at room temperature with horseradish peroxidase (HRP)–conjugated secondary antibody. After extensive washing in TTBS, the blots were developed using the LAS-1000 Single System (Fujifilm, Tokyo, Japan). Monoclonal antibodies against CAS (clone 24) and paxillin (clone 349) were obtained from BD Transduction Laboratories (Lexington, KY). Anti-FAK polyclonal rabbit antibody (FAK C-20), anti–Cas-L monoclonal mouse antibody (2G9), and HRP-conjugated anti-mouse and anti–rabbit immunoglobulin G were from Santa Cruz Biotechnology (Santa Cruz, CA). Anti-GST antibody was from Amersham Pharmacia Biotech (Piscataway, NJ). Anti–phosphotyrosine 4G10 was from Millipore (Billerica, MA). Phospho-specific antibodies against FAK phosphotyrosine (397, 861) were from

BioSource International (Camarillo, CA). Phospho-specific antibodies against CAS phosphotyrosine 410 and paxillin phosphotyrosine 118 were from Cell Signaling Technology (Beverly, MA).

CAS pY12 antibody was developed in collaboration with 21st Century Biochemicals (Marlboro, MA) by immunizing rabbits with synthetic peptide corresponding to residues surrounding mouse CAS Y12 tyrosine, CVLAKAL[pY]DNVAESP amide, respectively, where pY indicates phosphotyrosine. The peptide was synthesized with N-terminal cysteine residue and coupled to MBS for immunization. The antibody was affinity purified from rabbit antisera by affinity chromatography steps using protein A columns to purify immunoglobulins followed by specific immunodepletion using nonphosphopeptide and affinity purification using phosphopeptide (immunogen) columns to obtain the CAS pY12 affinity-purified antibody used in this study.

For immunoprecipitations, cells were lysed in NP-40 lysis buffer (50 mM Tris, pH 7.4, 150 mM NaCl, 1% NP-40, 5 mM EDTA, 50 mM NaF). Lysates containing 500 mg of proteins were incubated for 4 h on ice with 1 µg of primary antibody (FAK C- 20), and immune complexes were collected by additional 1-h incubation with protein A–Sepharose (20 µl of 50% slurry; Zymed, San Francisco, CA). The immunoprecipitates were washed five times with 1 ml of ice-cold NP-40 lysis buffer, resuspended in 2× SDS–PAGE sample buffer, and processed for immunoblotting.

GST pull-downs and phosphorylation reactions

Cell lysates were incubated with glutathione Sepharose 4B beads with immobilized GST or GST-CAS-SH3 variants at 4°C for 2 h. The beads were washed extensively and boiled in Laemmli sample buffer, and proteins were detected by SDS–PAGE and immunoblotting. Phosphorylation reactions of the CAS SH3-domain variants were conducted in 50 mM 4-(2-hydroxyethyl)-1-piperazineethanesulfonic acid, pH 7.4, containing 10 mM $MgCl_2$, 0.1 mM sodium orthovanadate, 2 mM dithiothreitol, and 0.1 mM ATP for 80 min at 30°C and initiated by adding 400 ng of recombinant Bmx kinase (Cell Signaling Technology).

Immunofluorescence microscopy

Cell were seeded on coverslips coated with human fibronectin 10 µg/ml (Invitrogen, Carlsbad, CA), grown for 24–48 h, and subsequently fixed in 4% paraformaldehyde, permeabilized in 0.5% Triton X-100, washed extensively with PBS, and blocked in 3% bovine serum albumin. The cells were then sequentially incubated with primary antibody for 2 h, secondary antibody for 60 min, and Alexa Fluor 594 phalloidin (Molecular Probes, Invitrogen) for 15 min, with extensive washing between each step. The primary antibodies were as follows: anti-phosphotyrosine (clone 4G10; Upstate, Millipore), anti-phosphopaxillin (Tyr118; Cell Signaling Technology), and anti-phosphocortactin (pY421; BioSource International). The secondary antibodies were as follows: anti-rabbit (Alexa 546) and anti-mouse (Alexa 594, Alexa 633; Molecular Probes). Images were acquired by a TCS SP2 microscope system (Leica, Wetzlar, Germany) equipped with a Leica 63×/1.45 oil objective.

In-gel gelatin zymography

Fifty thousand cells were plated per well of a 24-well dish. After 16 h, cells were washed with PBS and incubated in 300 µl of serum-free media for 24 or 72 h. Aliquots (30 µl) of the conditioned media were loaded for zymography on a 10% SDS–PAGE gel containing 1 mg/ml gelatin as described previously (Pozzi *et al.*, 2000). Briefly, gel proteins were washed for 1 h in 50 mM Tris-HCl (pH 7.5), 0.1 M NaCl, and 2.5% Triton X-100 and then incubated at 37°C in 50 mM Tris-HCl (pH 7.5), 10 mM $CaCl_2$, and 0.02% Na azide for 17 h. Gels were stained with Coomassie blue and destained in 7% acetic acid/5% methanol.

Alexa 633 gelatin zymography

To prepare Alexa Fluor 633 gelatin, 2 µl of Alexa 633 reactive dye (1 µg/ml; Molecular Probes) was conjugated with 1 ml of gelatin (10 mg/ml; Bio-Rad, Hercules, CA) diluted in 0.1 M sodium bicarbonate buffer, pH 9.0, for 30 min. The unconjugated dye was removed by passage through a Zeba Micro Desalt Spin Column (Thermo Scientific, Waltham, MA). Coverslips were coated with Alexa Fluor 633 gelatin (1 mg/ml), air dried, rehydrated with water for 15 min in 4°C, and fixed with 0.5% glutaraldehyde for 30 min in 4°C. RsK4 cells transfected with GFP-CAS were grown on Alexa Fluor 633 gelatin–coated coverslips for 24 h and then fixed in 4% paraformaldehyde, permeabilized in 0.5% Triton X-100, washed thrice with PBS, blocked in 3% bovine serum albumin, and mounted.

Migration assays

Cell migration was analyzed using the Oris Cell Migration Assay (Platypus Technologies, Madison, WI) with some modifications. The cell-seeding stopper was inserted into 96-well plate, and well bottoms were either uncoated (polylysine) or coated with 10 µg/ml fibronectin (Invitrogen). Fifty thousand cells were seeded into each well with a stopper to restrict cell seeding to the outer annular regions of the wells. Removal of the stopper results in opening of a round, unseeded region, into which the seeded cells migrate. Migration was assessed using Eclipse TE2000-S (4×/0.13 Plan Fluor objectives; Nikon, Melville, NY) mounted with a VDS Vosskühler CCD-1300 camera (Allied Vision Technologies, Osnabrück, Germany) as a decrease of cell-free area in time quantified by NIS-Elements software (Nikon). Alternatively, migration was analyzed according to manufacturer's protocol using an Ibidi Culture-Insert (Ibidi, Munich, Germany) in a 35-mm µ-Dish. Briefly, 70 µl of a cell suspension (7×10^5 cells/ml) was applied into each well and incubated at 37°C and 5% CO_2. After appropriate cell attachment was achieved (24 h), the Culture-Insert was removed and the µ-Dish was filled with cell-free medium (2 ml of media for 35-mm µ-Dish). Migration was also assessed, using a Nikon Eclipse TE2000-S (10×/0.25 Plan Fluor objective), as a decrease of cell-free area in time quantified by NIS-Elements software (Laboratory Imaging, Prague, Czech Republic).

Chemotaxis was analyzed using a Boyden chamber chemotaxis assay (BD Biosciences, Oxford, UK) according to the manufacturer's protocol. Briefly, 500 µl of media containing 10% fetal bovine serum was added to the lower chambers. A total of 10^5 cells suspended in 0.3 ml serum-free D-MEM was loaded to the top of each chamber and then incubated at 37°C in 5% CO_2. After 10 h, the chambers were washed with PBS. Cells were fixed in 4% paraformaldehyde in 1× PBS for 15 min and stained with 4′,6-diamidino-2-phenylindole. Representative fields were documented by fluorescence microscopy and the numbers of transmigrated cells determined from replicate chambers by counting 10 random areas at 200× magnification.

Spreading assays

Cells were trypsinized and counted, and 2.5×10^5 cells were added with medium to 100-mm culture dishes for a final volume of 10 ml. Random fields were photographed after 120 min using a low-magnification, phase-contrast microscope and evaluated for the percentage of spread cells. Unspread cells were apparent as phase-bright and punctual, whereas spread cells were not phase-bright, with extensive visible membrane protrusions. The two kinds of cells were

distinguishable such that two independent counts of the same field gave the same result ±2%. Three fields were counted for each cell line, and, in each field, >200 cells were counted. The experiment was repeated twice.

Invasion assays

Invasiveness of cells was analyzed using the Ibidi μ-Slide Angiogenesis System. A 200-μl solution containing 2 mg/ml collagen R (Serva, Heidelberg, Germany) and 4 mg/ml collagen G (Biochrom, Berlin, Germany) was prepared, and 46 μl of $NaHCO_3$ and 46 μl minimum essential medium Eagle (modified) with Hank's salts (HMEM) were added. A total of 10 μl of the collagen solution was added into each well of μ-Slide Angiogenesis plate and polymerized at 37°C. Fifty μl of cell suspension (2×10^5 cells/ml) was added on top of a collagen gel. After 2 d, invasion was scored as an average invasion depth of the cells in selected field of view using Nikon Eclipse TE2000-S (20×/0.45 Plan Fluor objective) and NIS Elements software. For each experiment six fields of view were analyzed by 10-μm optical sections.

Fluorescence recovery after photobleaching

FRAP studies were conducted on live cells expressing either GFP-tagged CAS or YFP-tagged vinculin. The cells were plated on glass-bottom dishes (MatTek, Ashland, MA) coated with 10 μg/ml fibronectin and cultured for 24 h before the experiment. Measurements were performed in DMEM at 37°C and 5% CO2. Ten focal adhesions and 10 podosome-type adhesions, each structure from a different cell, expressing GFP-CAS or YFP-vinculin was analyzed. After a brief measurement at monitoring intensity (488 nm), a high-energy beam was used to bleach 30–50% of the intensity in the spot. The intensity of recovery of the bleached region was extracted from the images series, and curves were fit to single-exponential functions. The characteristic fluorescence recovery time was extracted from the FRAP curves.

Statistical analysis

Statistical significances were determined using an unpaired, two-tailed, Student's *t* test.

ACKNOWLEDGMENTS

We thank Marie Charvátová for excellent technical assistance. This work was supported by Grant Agency of Charles University Grant 1310 and Czech Ministry of Education, Youth and Sport Grants LC06061 and MSM0021620858. We thank the reviewers for useful comments.

REFERENCES

Abassi YA, Rehn M, Ekman N, Alitalo K, Vuori K (2003). p130Cas couples the tyrosine kinase Bmx/Etk with regulation of the actin cytoskeleton and cell migration. J Biol Chem 278, 35636–35643.

Angers-Loustau A, Cote JF, Charest A, Dowbenko D, Spencer S, Lasky LA, Tremblay ML (1999). Protein tyrosine phosphatase–PEST regulates focal adhesion disassembly, migration, and cytokinesis in fibroblasts. J Cell Biol 144, 1019–1031.

Brabek J, Constancio SS, Shin NY, Pozzi A, Weaver AM, Hanks SK (2004). CAS promotes invasiveness of Src-transformed cells. Oncogene 23, 7406–7415.

Brabek J, Constancio SS, Siesser PF, Shin NY, Pozzi A, Hanks SK (2005). Crk-associated substrate tyrosine phosphorylation sites are critical for invasion and metastasis of SRC-transformed cells. Mol Cancer Res 3, 307–315.

Brinkman A, van der FS, Kok EM, Dorssers LC (2000). BCAR1, a human homologue of the adapter protein p130Cas, and antiestrogen resistance in breast cancer cells. J Natl Cancer Inst 92, 112–120.

Burridge K, Wennerberg K (2004). Rho and Rac take center stage. Cell 116, 167–179.

Chan KT, Cortesio CL, Huttenlocher A (2009). FAK alters invadopodia and focal adhesion composition and dynamics to regulate breast cancer invasion. J Cell Biol 185, 357–370.

Chen S, O'Reilly LP, Smithgall TE, Engen JR (2008). Tyrosine phosphorylation in the SH3 domain disrupts negative regulatory interactions within the c-Abl kinase core. J Mol Biol 383, 414–423.

Cho SY, Klemke RL (2000). Extracellular-regulated kinase activation and CAS/Crk coupling regulate cell migration and suppress apoptosis during invasion of the extracellular matrix. J Cell Biol 149, 223–236.

Defilippi P, Di Stefano P, Cabodi S (2006). p130Cas: a versatile scaffold in signaling networks. Trends Cell Biol 16, 257–263.

Donato DM, Ryzhova LM, Meenderink LM, Kaverina I, Hanks SK (2010). Dynamics and mechanism of p130Cas localization to focal adhesions. J Biol Chem 285, 20769–20779.

Dorssers LC, Grebenchtchikov N, Brinkman A, Look MP, Klijn JG, Geurts-Moespot A, Span PN, Foekens JA, Sweep CG (2004). Application of a newly developed ELISA for BCAR1 protein for prediction of clinical benefit of tamoxifen therapy in patients with advanced breast cancer. Clin Chem 50, 1445–1447.

Fonseca PM, Shin NY, Brabek J, Ryzhova L, Wu J, Hanks SK (2004). Regulation and localization of CAS substrate domain tyrosine phosphorylation. Cell Signal 16, 621–629.

Garton AJ, Burnham MR, Bouton AH, Tonks NK (1997). Association of PTP–PEST with the SH3 domain of p130cas; a novel mechanism of protein tyrosine phosphatase substrate recognition. Oncogene 15, 877–885.

Harte MT, Hildebrand JD, Burnham MR, Bouton AH, Parsons JT (1996). p130Cas, a substrate associated with v-Src and v-Crk, localizes to focal adhesions and binds to focal adhesion kinase. J Biol Chem 271, 13649–13655.

Honda H, Nakamoto T, Sakai R, Hirai H (1999). p130(Cas), an assembling molecule of actin filaments, promotes cell movement, cell migration, and cell spreading in fibroblasts. Biochem Biophys Res Commun 262, 25–30.

Huang J, Hamasaki H, Nakamoto T, Honda H, Hirai H, Saito M, Takato T, Sakai R (2002). Differential regulation of cell migration, actin stress fiber organization, and cell transformation by functional domains of Crk-associated substrate. J Biol Chem 277, 27265–27272.

Joseph RE, Fulton DB, Andreotti AH (2007). Mechanism and functional significance of Itk autophosphorylation. J Mol Biol 373, 1281–1292.

Kira M, Sano S, Takagi S, Yoshikawa K, Takeda J, Itami S (2002). STAT3 deficiency in keratinocytes leads to compromised cell migration through hyperphosphorylation of p130(cas). J Biol Chem 277, 12931–12936.

Kirsch KH, Georgescu MM, Hanafusa H (1998). Direct binding of p130(Cas) to the guanine nucleotide exchange factor C3G. J Biol Chem 273, 25673–25679.

Kiyokawa E, Hashimoto Y, Kobayashi S, Sugimura H, Kurata T, Matsuda M (1998a). Activation of Rac1 by a Crk SH3-binding protein, DOCK180. Genes Dev 12, 3331–3336.

Kiyokawa E, Hashimoto Y, Kurata T, Sugimura H, Matsuda M (1998b). Evidence that DOCK180 up-regulates signals from the CrkII–p130(Cas) complex. J Biol Chem 273, 24479–24484.

Klemke RL, Leng J, Molander R, Brooks PC, Vuori K, Cheresh DA (1998). CAS/Crk coupling serves as a "molecular switch" for induction of cell migration. J Cell Biol 140, 961–972.

Li X, Earp HS (1997). Paxillin is tyrosine-phosphorylated by and preferentially associates with the calcium-dependent tyrosine kinase in rat liver epithelial cells. J Biol Chem 272, 14341–14348.

Liu F, Sells MA, Chernoff J (1998). Transformation suppression by protein tyrosine phosphatase 1B requires a functional SH3 ligand. Mol Cell Biol 18, 250–259.

Luo W, Slebos RJ, Hill S, Li M, Brabek J, Amanchy R, Chaerkady R, Pandey A, Ham AJ, Hanks SK (2008). Global impact of oncogenic Src on a phosphotyrosine proteome. J Proteome Res 7, 3447–3460.

Meenderink LM, Ryzhova LM, Donato DM, Gochberg DF, Kaverina I, Hanks SK (2010). P130Cas Src-binding and substrate domains have distinct roles in sustaining focal adhesion disassembly and promoting cell migration. PLoS One 5, e13412.

Meyn MA, III, Wilson MB, Abdi FA, Fahey N, Schiavone AP, Wu J, Hochrein JM, Engen JR, Smithgall TE (2006). Src family kinases phosphorylate the Bcr-Abl SH3-SH2 region and modulate Bcr-Abl transforming activity. J Biol Chem 281, 30907–30916.

Mohl C, Kirchgessner N, Schafer C, Kupper K, Born S, Diez G, Goldmann WH, Merkel R, Hoffmann B (2009). Becoming stable and strong: the

interplay between vinculin exchange dynamics and adhesion strength during adhesion site maturation. Cell Motil Cytoskeleton 66, 350–364.
Morrogh LM, Hinshelwood S, Costello P, Cory GO, Kinnon C (1999). The SH3 domain of Bruton's tyrosine kinase displays altered ligand binding properties when auto-phosphorylated in vitro. Eur J Immunol 29, 2269–2279.
Nakamoto T, Sakai R, Honda H, Ogawa S, Ueno H, Suzuki T, Aizawa S, Yazaki Y, Hirai H (1997). Requirements for localization of p130cas to focal adhesions. Mol Cell Biol 17, 3884–3897.
Nakamoto T, Yamagata T, Sakai R, Ogawa S, Honda H, Ueno H, Hirano N, Yazaki Y, Hirai H (2000). CIZ, a zinc finger protein that interacts with p130(cas) and activates the expression of matrix metalloproteinases. Mol Cell Biol 20, 1649–1658.
Nojima Y, Morino N, Mimura T, Hamasaki K, Furuya H, Sakai R, Sato T, Tachibana K, Morimoto C, Yazaki Y (1995). Integrin-mediated cell adhesion promotes tyrosine phosphorylation of p130Cas, a Src homology 3–containing molecule having multiple Src homology 2–binding motifs. J Biol Chem 270, 15398–15402.
Park H, Wahl MI, Afar DE, Turck CW, Rawlings DJ, Tam C, Scharenberg AM, Kinet JP, Witte ON (1996). Regulation of Btk function by a major autophosphorylation site within the SH3 domain. Immunity 4, 515–525.
Polte TR, Hanks SK (1995). Interaction between focal adhesion kinase and Crk-associated tyrosine kinase substrate p130Cas. Proc Natl Acad Sci USA 92, 10678–10682.
Polte TR, Hanks SK (1997). Complexes of focal adhesion kinase (FAK) and Crk-associated substrate (p130(Cas)) are elevated in cytoskeleton-associated fractions following adhesion and Src transformationRequirements for Src kinase activity and FAK proline-rich motifs. J Biol Chem 272, 5501–5509.
Pozzi A, Moberg PE, Miles LA, Wagner S, Soloway P, Gardner HA (2000). Elevated matrix metalloprotease and angiostatin levels in integrin alpha 1 knockout mice cause reduced tumor vascularization. Proc Natl Acad Sci USA 97, 2202–2207.
Ruest PJ, Shin NY, Polte TR, Zhang X, Hanks SK (2001). Mechanisms of CAS substrate domain tyrosine phosphorylation by FAK and Src. Mol Cell Biol 21, 7641–7652.
Sakai R, Iwamatsu A, Hirano N, Ogawa S, Tanaka T, Nishida J, Yazaki Y, Hirai H (1994). Characterization, partial purification, and peptide sequencing of p130,the main phosphoprotein associated with v-Crk oncoprotein. J Biol Chem 269, 32740–32746.
Shin NY, Dise RS, Schneider-Mergener J, Ritchie MD, Kilkenny DM, Hanks SK (2004). Subsets of the major tyrosine phosphorylation sites in Crk-associated substrate (CAS) are sufficient to promote cell migration. J Biol Chem 279, 38331–38337.
Siesser PM, Meenderink LM, Ryzhova L, Michael KE, Dumbauld DW, Garcia AJ, Kaverina I, Hanks SK (2008). A FAK/Src chimera with gain-of-function properties promotes formation of large peripheral adhesions associated with dynamic actin assembly. Cell Motil Cytoskeleton 65, 25–39.
Tolde O, Rosel D, Mierke CT, Pankova D, Folk P, Vesely P, Brabek J (2010a). Neoplastic progression of the human breast cancer cell line G3S1 is associated with elevation of cytoskeletal dynamics and upregulation of MT1-MMP. Int J Oncol 36, 833–839.
Tolde O, Rosel D, Vesely P, Folk P, Brabek J (2010b). The structure of invadopodia in a complex 3D environment. Eur J Cell Biol 89, 674–680.
Vesely P (1972). Tumour cell surface specialization in the uptake of nutrients evidenced by cinemicrography as a phenotypic condition for density independent growth. Folia Biol (Praha) 18, 395–401.
Vuori K, Hirai H, Aizawa S, Ruoslahti E (1996). Introduction of p130cas signaling complex formation upon integrin–mediated cell adhesion: a role for Src family kinases. Mol Cell Biol 16, 2606–2613.
Vuori K, Ruoslahti E (1995). Tyrosine phosphorylation of p130Cas and cortactin accompanies integrin-mediated cell adhesion to extracellular matrix. J Biol Chem 270, 22259–22262.
Webb DJ, Donais K, Whitmore LA, Thomas SM, Turner CE, Parsons JT, Horwitz AF (2004). FAK-Src signalling through paxillin, ERK and MLCK regulates adhesion disassembly. Nat Cell Biol 6, 154–161.
Wisniewska M, Bossenmaier B, Georges G, Hesse F, Dangl M, Kunkele KP, Ioannidis I, Huber R, Engh RA (2005). The 1.1 A resolution crystal structure of the p130cas SH3 domain and ramifications for ligand selectivity. J Mol Biol 347, 1005–1014.